COBEM 2023 27TH INTERNATIONAL CONGRESS OF MECHANICAL ENGINEERING

ABCM Brazilian Society of Mechanical Sciences and Engineering
27th ABCM International Congress of Mechanical Engineering
December 04-08, 2023, Florianópolis-SC, Brazil

COB-2023-2076
PRELIMINARY ANALYSIS ON THE EFFECTS OF THERMAL AGING AND CORROSION ON OPTICAL AND MORPHOLOGICAL PROPERTIES OF CHROMIUM-BASED ABSORBER SURFACES DEPOSITED BY MAGNETRON SPUTTERING

Thaís de Oliveira Almeida
Kelly Cristiane Gomes
Universidade Federal da Paraíba, Campus I, Lot. Cidade Universitaria, PB, 58051-900
toalmeida.engmec@gmail.com, gomes@cear.ufpb.br

Francielle Cristine Gonçalves
Universidade Federal da Paraíba, Campus I, Lot. Cidade Universitaria, PB, 58051-900
franciellycristine7@gmail.com

Flávia de Medeiros Aquino
Universidade Federal da Paraíba, Campus I, Lot. Cidade Universitaria, PB, 58051-900
flavia@cear.ufpb.br

Abstract. *Solar energy has a great potential as an alternative renewable source, even if, through photothermic conversion, it is being utilized in small scale due to limitations in applicability of solar collectors. In this context, the solution is to use them coated with selective surfaces, so they can absorb as much as possible of the solar radiation and emit the least possible heat. The present work has the objective to start a study of the effects of thermal aging and of the durability under corrosive environments on chromium-based absorber surfaces. Two multilayer solar surfaces are being studied (Cr_2O_3 – Cr/Cr_2O_3 and Cr_2O_3 – Cr/Cr_2O_3 – SiO_2), deposited by Magnetron Sputtering in stainless steel AISI 304 surface-treated with electropolishing. To this date, all samples were characterized optically and morphologically using UV-Vis-NIR Spectrophotometry and Infrared Spectroscopy before the customized thermal aging tests. The randomly chosen samples to be studied on room temperature had their chemical stabilities analyzed under corrosive environment by linear potentiodynamic polarization and chemical impedance spectroscopy. Preliminary analyses show that the presence of SiO_2 doesn't interfere on the absorptance, even if the difference between the values of band-gaps suggests otherwise. This requires further investigation of the emittance and selectivity to analyze if the SiO_2 interferes or not on the applicability of the surfaces. After the corrosion test, the sample with the SiO_2 layer presented a better result on chemical resistance, as the surface is almost intact after being exposed to the corrosive environment.*

Keywords: *selective surface, magnetron sputtering, thermal ageing, corrosion, durability*

1. INTRODUCTION

Throughout history, it has been known that energy consumption is an important factor for the socioeconomic development of societies. However, the current energy consumption system, heavily based on fossil fuels, is becoming increasingly unsustainable — due to the reduction of such sources and, for example, the emission of greenhouse gases. Therefore, technological developments are necessary to reduce this dependence and the impact on the environment (KHAN et al., 2022; MEDIAVILLA et al., 2013). Thus, the focus shifts to alternative and renewable energy, originated from natural processes with high replacement rates, namely: solar energy; wind power; geothermal energy; hydropower; marine power; and bioenergy — biomass and biofuels (BHATTACHARYA et al., 2016; GIELEN et al., 2019).

Among all sources, solar energy may be the best option for the future because of the following factors: it is the most abundant source of energy, as the Sun emits 3.8×10^{23} kWh, of which 1.8×10^{14} are intercepted by the Earth in diverse forms (such as light and heat), and this amount is capable of supplying the planet's energy needs at no cost; it is an inexhaustible source of energy, with high utilization efficiencies, especially suitable for developing countries (thanks to high values of density and radiation intensity); there are no negative environmental impacts from its use; it can be efficiently used in small, medium and large scale with high efficiency maintenance (KANNAN; VAKEESAN, 2016; RABAIA et al., 2021). In Brazil, the primary source of energy is the hydropower, but in drought occurrences, there is the need to activate thermoelectric power plants. To mitigate this, it is important to invest in and use more of, but not limited to, solar energy applications to take advantage of the country's high solar irradiation rates (COSTA et al., 2021).

Solar energy can be used in photothermal, photovoltaic and photocatalytic applications (GONG; LI; WASIELEWSKI, 2019). Solar thermal energy — that is, solar radiation directly used to generate heat —can be used in both low and high temperature applications. For its use, solar collectors are needed, a special type of heat exchanger that absorbs solar radiation, converts it into heat and transfers that energy to a fluid of interest (GORJIAN et al., 2020). However, even with a good cost-benefit ratio, for temperatures above 100 °C, limitations are perceived in the applicability of solar collectors for two reasons: the higher the temperature of the collector, the greater the amount of heat emitted by radiation; and the materials that compose it must have thermomechanical stability under these conditions (SILVA NETO, 2017).

Considering the emission of heat by radiation as a surface phenomenon (BERGMAN; LAVINE, 2019), solar collectors can be coated with materials that are good absorbers of radiation in the solar spectrum and bad emitters of heat in the spectral range of longer wavelengths (associated with the temperatures at which these collectors operate) at the same time. These coatings are called solar selective surfaces, or SSS (TABOR, 1961). To improve the relation between absorptivity and emissivity of SSS, and consequently the performance of solar collectors, the following can be done: use of materials with appropriate absorbing properties; overlapping of different coatings; surface texturing, thus creating optical traps; construction of films from cermet composite materials; and combinations of all these possibilities (SILVA NETO, 2017).

To produce efficient and durable selective surfaces they must have high thermomechanical stability between layers, by themselves and combined, and excellent adhesion between layers and substrate (XU et al., 2020). Beyond those requirements, the surfaces also need to be resistant to oxidation, humidity, atmospheric corrosion, diffusion processes and chemical reactions (HU et al., 2019). Therefore, the choice of materials and deposition methods need to be made carefully and taking in consideration the application of the selective surfaces.

A variety of deposition methods can be utilized to produce selective surfaces for medium and high temperatures of operation, such as chemical vapor deposition, electroplating, inorganic pigmentation of anodized aluminum and physical vapor deposition (BELLO; SHANMUGAN, 2020). One of the methods classified as the latter is the magnetron sputtering. This method utilizes a magnetic field parallel to the target's surface, limiting the secondary electrons' movements. The containment of those electrons increases the probability of ionizing collisions between electrons and atoms, increasing the density of the plasma close to the surface of the target. Consequently, the pulverization rate of the target is higher and so is the deposition rate on the substrate, under lower work pressures and voltages (GUDMUNDSSON, 2020).

Another factor to be taken in consideration regarding the use of selective surfaces is its work environment, because external agents can negatively affect their properties. The operation temperatures and the heating/cooling cycles, also known as thermal aging, can reduce the collector's efficiency and its service time (ZHANG et al., 2017). Also, materials inherently interact with the environment and it can compromise the materials' integrity. One of those interactions is the corrosion, defined by the deterioration or destruction of a component (CALLISTER JR; RETHWISCH, 2016).

For solar collectors, corrosion resistance is a universal problem derived from the association of selective surface long life stability and solar energy/heat conversion efficiency (KOŽELJ et al., 2009). Atmospheric corrosion is one of the major causes of selective surface failure (YU et al., 2020), since the air exposure leads to chemical diffusion between layers, formation of oxide files and negative interactions of humidity with the surface (KUMAR; DIXIT, 2019). However, this problem is not easy to be solved, as the protection layers against corrosion cannot hinder the film's selectivity (KOŽELJ et al., 2009). Therefore, anti-reflective layers can be used as protective layers (ŠEST et al., 2018).

Thus, the present work aims to start a study on the effects of thermal aging and corrosive environments on chromium-based solar absorbing surfaces obtained by the Magnetron Sputtering method, analyzing optical and chemical properties to understand the behavior deposited films.

2. MATERIALS AND METHODS

In order to achieve the objectives of the entire research, the experimental program is detailed below:

1. Preparation of substrates (28 samples, 24 for deposition and 4 for reference);
2. Deposition of thin films on substrates (12 specimens for the Cr_2O_3 – Cr/Cr_2O_3 film and 12 specimens for the Cr_2O_3 – Cr/Cr_2O_3 – SiO_2 film);
3. Characterization of films;
4. Thermal treatment of specimens (3 of each film + 1 reference substrate for each chosen temperature);
5. Characterization of surfaces after heat treatment;
6. Corrosion analysis of produced surfaces (before and after heat treatment);
7. Characterization of surfaces after corrosion tests.

2.1 Materials

For the present work, black chromium was selected as the absorbing layer and silica as the anti-reflective layer, both deposited by the Magnetron Sputtering method, as justified in the following sections.

Absorbing layer

Among the most common materials for selective surfaces, black chromium (the Cr/Cr_2O_3 complex) has been used on a large scale, as it has the best thermal stability up to 400 °C. Laboratory studies have already shown that surfaces of this material have absorptivity between 0.95 and 0.96 and emissivity between 0.08 and 0.14, while line products have absorptivity of 0.94 and emissivity of 0.08 (CAO et al., 2014; DUFFIE; BECKMAN, 2013; KENNEDY, 2002).

Anti-reflective layer

The absorptivity of selective surfaces can be improved by using interference phenomena. Some layers that can be used on substrates with high values of reflectivity are semiconductors, which have high absorptivity in the solar spectrum. Amorphous silicon dioxide, or silica, has been widely used as an anti-reflective layer because it is resistant to abrasion and a durable material. It can also be used in cermets as a dielectric layer due to its high thermochemical stability (CAO et al., 2014; DUFFIE; BECKMAN, 2013; RAUT et al., 2011).

2.2 Substrate preparation

To carry out the present study, square substrates (30 x 30 x 0.5 mm) of stainless steel AISI 304 were used. Before deposition, the substrates underwent a surface electropolishing, a process used on a large industrial scale to obtain shiny and tension-free surfaces with low surface roughness (LIN; HU, 2008).

This process was carried out in a beaker containing a solution of phosphoric acid, sulfuric acid and glycerol in the volumetric proportion of 2:2:1 (by volume), and using a mesh (80 x 300 mm) made of the same stainless steel as the substrates to close the circuit. The substrates were completely submerged in the solution in the center of the beaker as the positive pole, with the mesh as the negative pole, both connected to a direct current power supply.

To stabilize the current, a sacrificial substrate was the first to be submitted to the process, with the power supply configured at 6 V. As soon as the current reached a level of 1.5 A, the substrates underwent the process for 10 minutes one by one. After, each sample was washed with distilled water and dried with absorbent paper, and all were stored in a polyethylene envelope with hermetic closure until the next process.

Then, all samples were submitted to an ultrasonic bath in isopropyl alcohol for 15 minutes, to remove traces of the electropolishing solution. Finally, the substrates were washed one at a time with distilled water and dried with hot air. Before being stored in hermetically sealed polyethylene envelopes for deposition, adhesive tape was placed on one end of each of the substrates to prevent deposition and, subsequently, to be used to measure the thickness of the film.

2.3 Cathodic deposition

The deposition process was carried out in a Magnetron Sputtering Orion 5 system, manufactured by AJA International Inc.

For all layers of the two absorber surface configurations, the substrates were placed on the support 106 mm away from the targets. The targets used were all supplied by Macashew Tecnologias LTDA, with 2" diameter and 3.5 mm thick. The SiO_2 target is 99.99% pure, while the Cr_2O_3 and Cr/Cr_2O_3 (40/60% by weight) targets are 99.95%.

The chamber was evacuated to a pressure of approximately $1x10^{-5}$ Torr for the injection of an inert gas, which was argon for all processes, until the internal pressure reached the level of $5x10^{-3}$ Torr. The radio frequency power source was turned on for the opening of the plasma, but not at the working power for all materials, which was 60 W. Initially, the value of 10 W was set, and the power was increased at a speed of 5 W/min until its final value. Throughout the process, the argon pressure was checked for plasma maintenance and stability.

The deposition of all layers lasted 2 hours each. At the end, the power was reduced in the same way that it was increased, 5 W/min between 60 and 10 W, before following with the total shutdown procedures of the deposition system. The chamber, after each process, was opened after 24 hours and as soon as the layers reached their final configurations, all samples were stored in polyethylene envelopes with hermetic closure.

Table 1 lists the summary of deposition parameters and the nomenclature adopted for each sample.

Table 1. Nomenclature adopted for samples and deposition parameters.

Sample	Layers	Power	Time	Future Thermal Aging Temperature (°C)
A25	Cr_2O_3 Cr/Cr_2O_3	60 W	2 hours	25
A200				200
A350				350
A500				500
B25	Cr_2O_3			25

B200	Cr/Cr_2O_3 SiO_2			200
B350				350
B500				500

The letter A refers to the Cr_2O_3 – Cr/Cr_2O_3 film and the letter B refers to the Cr_2O_3 – Cr/Cr_2O_3 – SiO_2 film. The value right after the first letter corresponds to the temperature to be adopted in the subsequent customized thermal aging tests (25 [for room temperature], 200, 350 and 500 °C). This nomenclature is adopted on Table 2 and on the labels of Figures 1, 2 and 3.

2.4 Characterization of the films

In the present work, only a few of the characterizations were executed to conduct the preliminary analysis.

UV-Vis-NIR Spectrophotometry

The equipment used to measure the absorption of the films was a Spectrophotometer in the Ultraviolet and Visible region and part of the Near Infrared (UV-Vis-NIR), manufactured by Shimadzu, model UV-2600. Operating in the region from 220 to 1400 nm in reflectance mode, this characterization was used to determine the reflectance of the films. With these results, the absorbances and the mean total solar absorptances of all samples were calculated.

Fourier-transform Infrared Spectroscopy (FTIR)

This characterization had the objective to complement the chemical characterization of the coatings based on the identification of the spectral regions where specific molecular absorption peaks occur. The equipment used in this analysis was an Infrared Spectrometer IR-Tracer 100 with full scanning range (NIR-MID-FIR), manufactured by Shimadzu, with spectroscopy in the mid-infrared (MID) range in Attenuated Total Reflectance (ATR) mode with the spectral range from 4000 cm^{-1} (~2500 nm) to 600 cm^{-1} (~16700 nm) in transmittance.

2.5 Corrosion process

For this test, an electrochemical cell with an aqueous sodium chloride electrolyte (concentration of 3.5% by weight) and three electrodes were used: Ag/AgCl as the reference electrode, platinum mesh as the counter electrode and samples as the working electrodes. The method used was linear potentiodynamic polarization and chemical impedance spectroscopy, using a compact potentiostat/galvanostat Autolab unit, manufactured by Metrohm. The polarization curves were obtained with a sweep rate of 1 mV/s and the impedance spectra were obtained with a frequency range from 10 kHz to 0.004 Hz and an amplitude of 0.01 V.

3. RESULTS AND DISCUSSIONS

3.1 UV-Vis

The total absorbance spectra of the manufactured films can be seen in Figure 1.

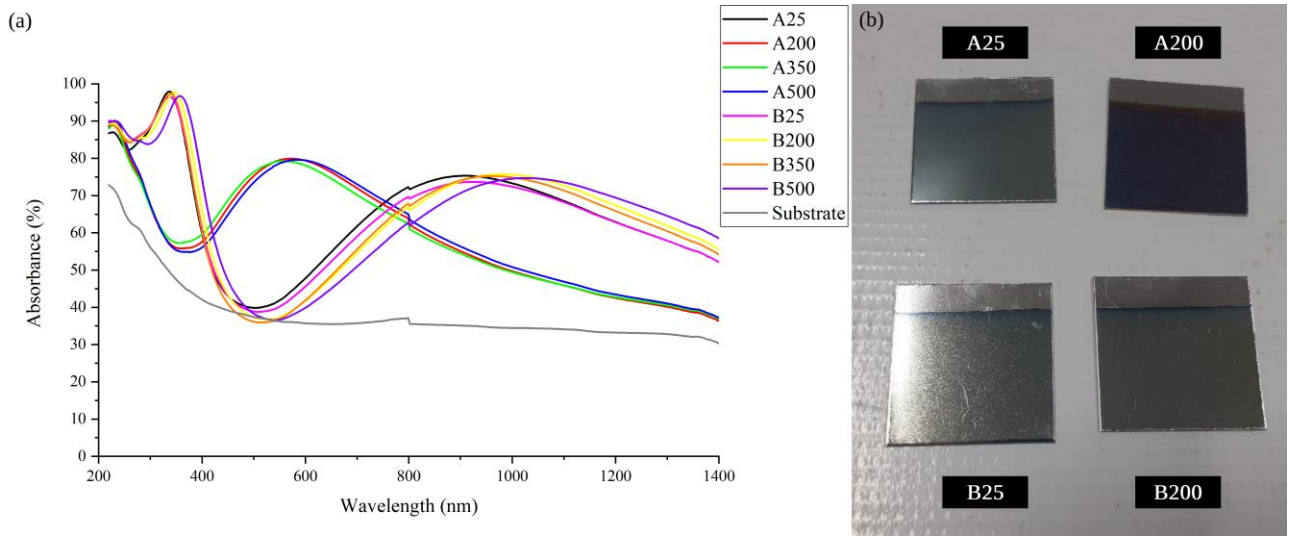

Figure 1. (a) Absorption spectra of the samples produced and (b) photographs of selected identified samples.

In general, all films showed better absorbance spectra than the pure substrate only superficially treated, with average solar absorptance (α) values listed in Table 2, corroborating what can be seen graphically. The difference in behavior between the A25 film and all others with the same configuration is due to the manufacture in two different cycles. More will be discovered and explained about the microstructural differences with subsequent characterizations. However, the values of absorptances differ from the consulted works (CAO et al., 2014; DUFFIE; BECKMAN, 2013; KENNEDY, 2002), as the films' colors deviate from the expected black.

The difference between the films without and with the anti-reflective layer still cannot be perceived, because of the close values of mean total solar absorptances. In this case, only the measure of emissivity and the calculi of selectivity can indicate if there is an improvement in the performance of the deposited films.

Table 2. Mean total solar absorptances and standard deviations for the produced samples.

Sample	α Mean (%)	Standard Deviation (%)
Substrate	36.54	1.30
A25	59.30	1.61
A200	64.40	0.82
A350	64.14	0.28
A500	64.65	0.39
B25	57.93	0.52
B200	57.26	0.40
B350	56.65	0.66
B500	56.64	0.94

Even with samples being manufactured at different stages, the deposition process has high reproducibility due to low standard deviations.

3.2 FTIR

The infrared spectra of the films can be seen in Figure 2.

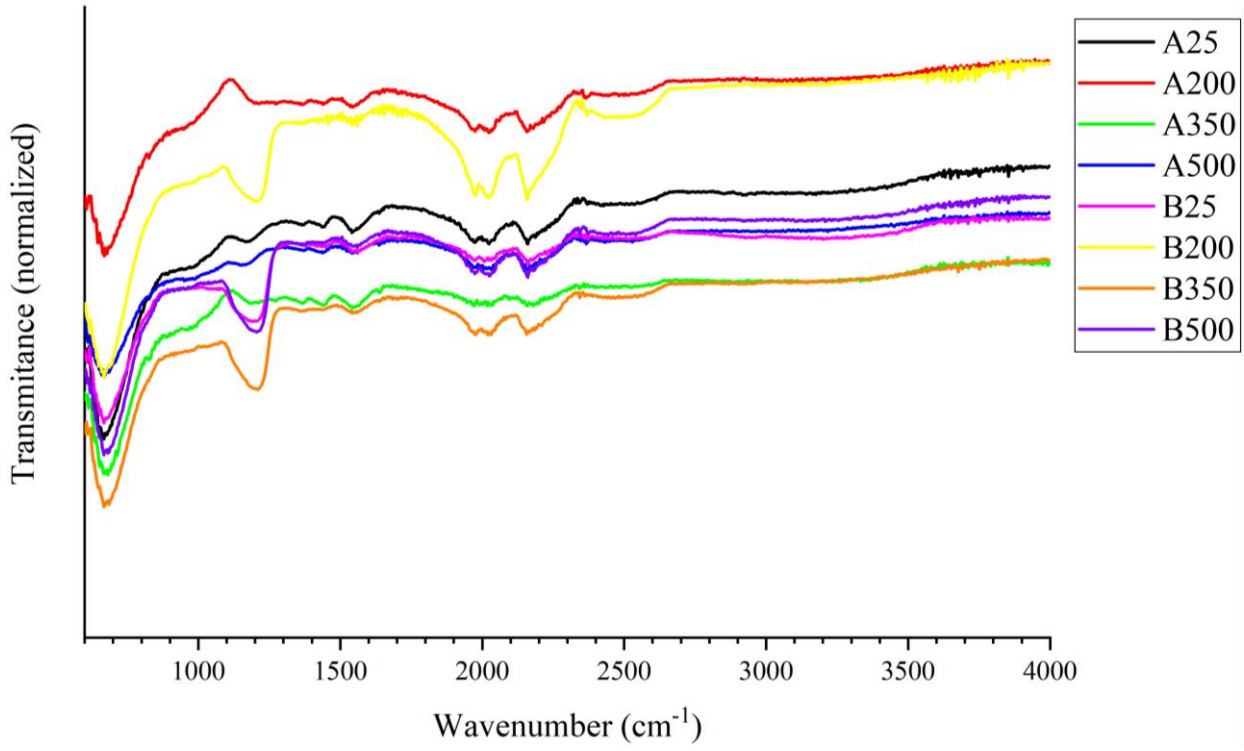

Figure 2. Infrared spectra of the samples produced.

The spectra of all films have a peak at ~700 cm^{-1} that confirms the presence of chromium oxide (Cr_2O_3) (PALERMO et al., 2019), since this material is present and prominent in the first two layers of both film configurations — in full in the first layer and as a composite in the second. The spectra of all B samples have a peak at ~1200 cm^{-1} for the vibration and asymmetric stretching of the Si–O–Si bond, characterizing the presence of silicon dioxide (SiO_2) (LI et al., 2013; LIPPINCOTT et al., 1958). Therefore, the deposition of the anti-reflective layer on the selected samples was successful. Identified in the spectra of all films, the bands between 1900 and 2200 cm^{-1} are related to the KBr crystal in the FTIR equipment system, as described in its technical manual. The spectra of all films have a peak at ~2350 cm^{-1}, and it is related to carbon dioxide (CO_2) present in the air and identified by the spectrophotometer during characterizations (BHARATHY; RAJI, 2018; SCHÄDLE; PEJCIC; MIZAIKOFF, 2016).

3.3 Preliminary calculations of band-gaps

It is possible to estimate the values of the spacing between bands with the absorption spectra and the thickness of the manufactured films. For preliminary studies of the samples produced and selected to be studied on room temperature, the spectra obtained with the UV-Vis analysis were used. However, even without measuring the thickness of the films, an estimate of this value was made from other works (GONÇALVES, 2021; OLIVEIRA, 2021) carried out with similar conditions for the same materials studied in the present work.

Finally, the Tauc method was used to obtain the curves considering direct transitions (FAN et al., 2021; RANI et al., 2017; TSEGAY; GEBRETINSAE; NURU, 2021), and the intersection on the x-axis of the extrapolation of the straight section of the curves gave the value of the band-gap.

The curves obtained for the manufactured films can be seen in Figure 3.

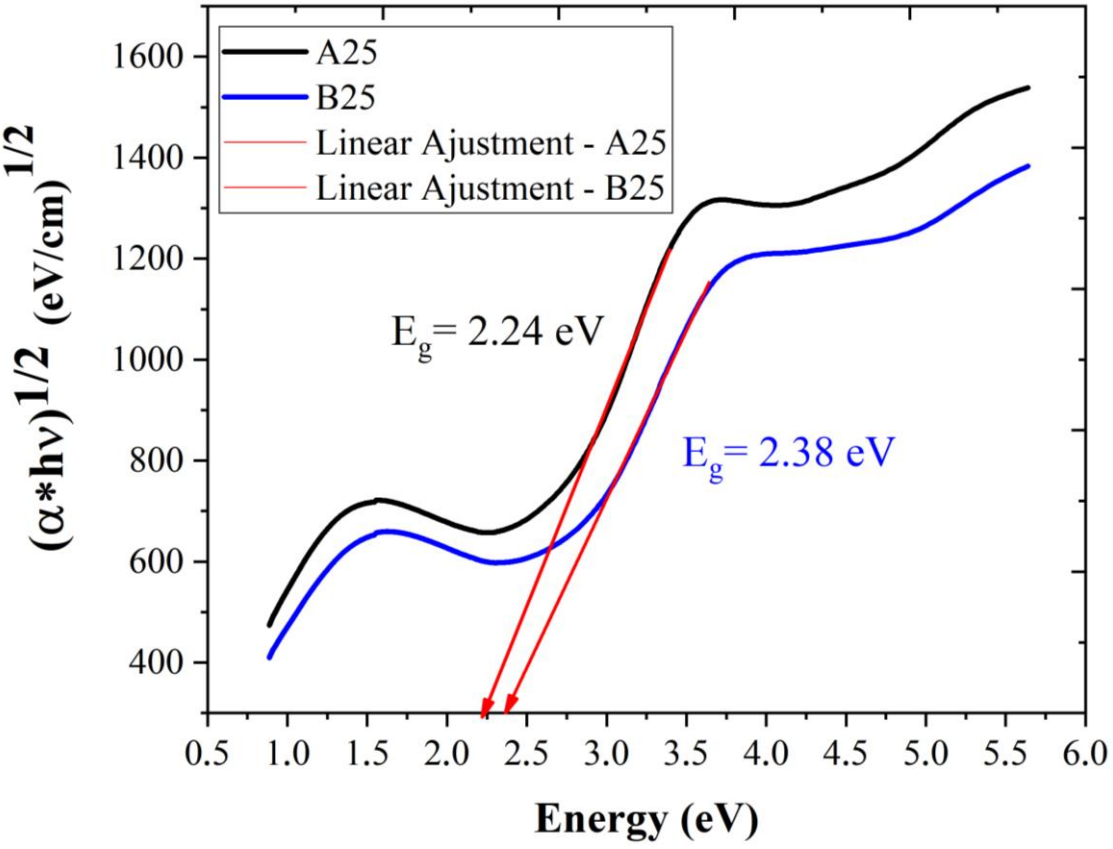

Figure 3. Band-gaps of two produced samples.

The band-gap values are consistent with consulted works (FAN et al., 2021; SILVA NETO, 2017; TSEGAY; GEBRETINSAE; NURU, 2021), even with the supposition of the thicknesses of the films. The decrease of the A film band-gap might be related to the presence of metallic chromium in its structure. The contrary happened to the B film, because the band-gap of silica is higher than the band-gap of chromium oxide. This behavior is consistent with the variation on the absorbance values, as listed on Table 2.

3.4 Preliminary observations of corrosion stability

The polarization curves of the preliminary corrosion tests and photographs of the samples for the two films selected to be studied on room temperature can be seen on Figure 4.

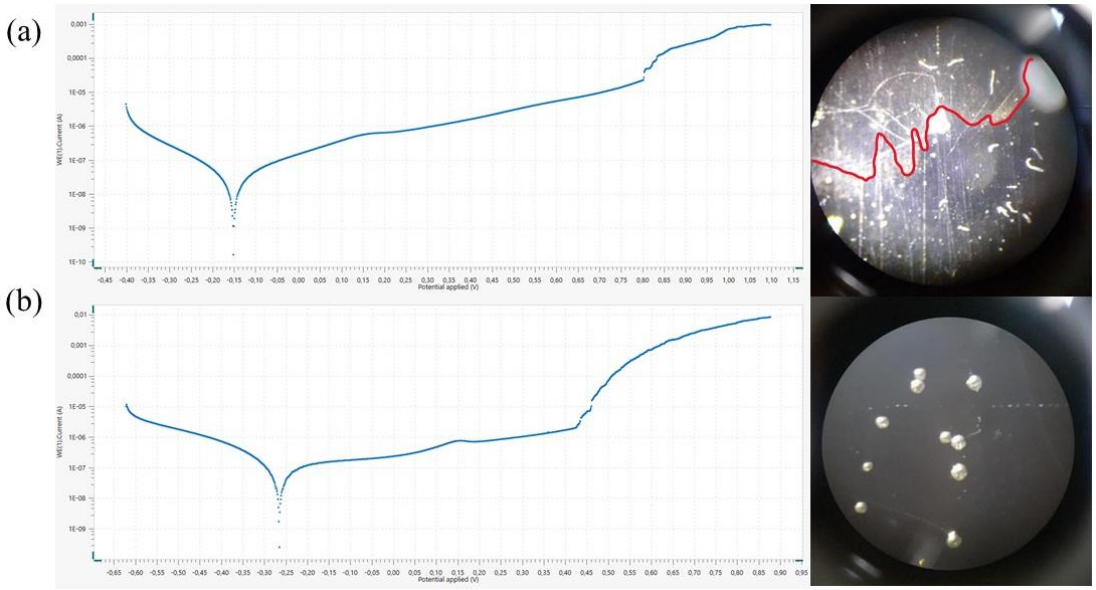

Figure 4. Polarization curves (current density *versus* potential) and photographs of the (a) A film and (b) B film.

By the Tafel extrapolation, the values of corrosion current and potential were calculated (QIAO et al., 2021). For the A film, the values are 0.48×10^{-7} A and -0.40 V respectively. For the B film, the values are 1.58×10^{-7} A and -0.64 V respectively. However, the values deviated from the expected, because a smaller corrosion current or greater corrosion potential corresponds to higher corrosion resistance (LIU et al., 2022). It is worth noting that being just a test, the same electrolyte was used for both samples — first for the A film and then for the B film. Therefore, the presence of ions might have had a negative influence on the corrosion values for the B film. Lastly, while the A film eroded completely in the corrosion process — the region above the red line on Figure 4(a) —, the B film resisted better, showing only signs of pitting — as seen on Figure 4(b). This can be attributed to the capacity of silica to form amorphous layers in high temperatures, what leads to less grain boundaries, and to better resist to corrosion processes as a consequence (HERRMANN; KLEMM, 2014).

4. CONCLUSION

All films exhibited higher mean total solar absorptances than the substrate that was only surface treated. However, the difference between the films with and without the anti-reflective layer has not yet been noticed due to the similar absorptances values. Therefore, the films with the anti-reflective layer present themselves as the better option to the intended application, thanks to its protective layer. Regarding the infrared spectra, the relevant peaks confirm the presence and successful deposition of the materials selected for analysis, making the Magnetron Sputtering an adequate deposition method. The band-gap calculi show that even with the presence of silica, what increases the band-gap value, the film still presents a behavior expected for an adequate absorbent coating. The preliminary corrosion tests show that the presence of silica impacts positively on the chemical resistance without changing the optical characteristics of the films, showing that it is a viable option to increase films' durability. Finally, the characterizations were essential to start the evaluation of the effects of the thermal and chemical stability of the films and their influence on their absorptivity.

5. ACKNOWLEDGEMENTS

We thank Profs. Drs. Kelly Cristiane Gomes e Flávia de Medeiros Aquino, of the *Laboratório de Filmes Finos* – LabFilm (DEER/UFPB), for providing the space and equipment used to conduct this study. This work has financial support of CAPES.

6. REFERENCES

BERGMAN, T.L.; LAVINE; A. S. Incropera - Fundamentals of Heat and Mass Transfer. 8. ed. Rio de Janeiro: LTC, 2019.

BHARATHY, G.; RAJI, P. Pseudocapacitance of Co doped NiO nanoparticles and its room temperature ferromagnetic behavior. Physica B: Condensed Matter. v. 530, p. 75–81, 2018.

BHATTACHARYA, M. et al. The effect of renewable energy consumption on economic growth: Evidence from top 38 countries. Applied Energy. v. 162, p. 733-741, 2016.

BELLO, M.; SHANMUGAN, S. Achievements in mid and high-temperature selective absorber coatings by physical vapor deposition (PVD) for solar thermal Application-A review. Journal of Alloys and Compounds. v. 839, 2020.

CALLISTER JR, W. D.; RETHWISCH, D. G. Ciência e engenharia de materiais: uma introdução. 9. ed. Rio de Janeiro: LTC, 2016.

CAO, F; McENANEY, K.; CHEN, G.; REN, Z. A review of cermet-based spectrally selective solar absorbers. Energy & Environmental Science. v. 7, p. 1615-1627, 2014.

COSTA, M. V. C. V.; CARVALHO, O. L. F.; ORLANDI, A. G.; HIRATA, I.; ALBUQUERQUE, A. O.; SILVA, F. V.; GUIMARÃES, R. F.; GOMES, R. A. T.; CARVALHO JÚNIOR, O. A. Remote Sensing for Monitoring Photovoltaic Solar Plants in Brazil Using Deep Semantic Segmentation. Energies. v. 14(10), 2021.

DUFFIE, J.A.; BECKMAN, W. A. Solar Engineering of Thermal Processes, Photovoltaics and Wind. Hoboken: John Wiley & Sons, Inc., 2013.

FAN, Z.; ZHU, M.; PAN, S.; GE, J.; HU, L. Giant photoresponse enhancement in Cr_2O_3 films by Ni doping-induced insulator-to-semiconductor transition. Ceramics International. v. 47, p. 13655-13659, 2021.

GIELEN, D.; BOSHELL, F.; SAYGIN, D.; BAZILIAN, M. D.; WAGNER, N; GORINI, R. The role of renewable energy in the global energy transformation. Energy Strategy Reviews. v. 24, p. 38-50, 2019.

GONÇALVES, K. S. Efeito do envelhecimento acelerado nas propriedades ópticas, morfológicas e microestruturais de superfícies absorvedoras multicamadas a base de cromo e sílica. Dissertation (Master in Renewable Energies) – Federal University of Paraíba, João Pessoa, 2021.

GONG, J.; LI, C.; WASIELEWSKI, M. R. Advances in solar energy conversion. Chemical Society Reviews. v. 48, p. 1862-1864, 2019.

GORJIAN, S.; EBADI, H.; CALISE, F.; SHUKLA, A.; INGRAO, C. A review on recent advancements in performance enhancement techniques for low-temperature solar collectors. Energy Conversion and Management. v. 222, 2020.

GUDMUNDSSON, J. T. Physics and technology of magnetron sputtering discharges. Plasma Sources Science and Technology. v. 29, 2020.

HERRMANN, M.; KLEMM, H. Corrosion of Ceramic Materials. In: SARIN, V. K. (Ed.). Comprehensive Hard Materials. v. 2, p. 413-446, 2014.

HU, C.; GUO, K.; LI, Y.; GU, Z.; QUAN, J.; ZHANG, S.; ZHENG, W. Optical coatings of durability based on transition metal nitrides. Thin Solid Films. v. 688, 2019.

KANNAN, N.; VAKEESAN, D. Solar energy for future world: - A review. Renewable and Sustainable Energy Reviews. v. 62, p. 1092-1105, 2016.

KENNEDY, C. E. Review of Mid- to High-Temperature Selective Solar Absorber Materials, NREL/TP-520-31267, National Renewable Energy Laboratory, Colorado, July 2002.

KHAN, A. A.; KHAN, S. U.; ALI, M. A. S.; SAFI, A.; GAO, Y.; LUO, J. Identifying impact of international trade and renewable energy consumption on environmental quality improvement and their role in global warming. Environmental Science and Pollution Research. v. 29, p. 33935–33944, 2022.

KOŽELJ, M.; VUK, A. Š.; JERMAN, I.; OREL, B. Corrosion protection of Sunselect, a spectrally selective solar absorber coating, by (3-mercaptopropyl)trimethoxysilane. Solar Energy Materials & Solar Cells. v. 93, p. 1733-1742, 2009.

KUMAR, R.; DIXIT, A. Corrosion resists Ni, Co co-pigmented nanoporous anodized alumina as spectral selective coating structure for solar thermal applications. Journal of Alloys and Compounds. v. 810, 151833, 2019.

LI, M.; ZENG, L.; CHEN, Y.; ZHUANG, L.; WANG, X.; SHEN, H. Realization of Colored Multicrystalline Silicon Solar Cells with SiO_2/SiN_x:H Double Layer Antireflection Coatings. International Journal of Photoenergy. v. 2013, p. 1-8, 2013.

LIN, C.-C.; HU, C.-C. Electropolishing of 304 stainless steel: Surface roughness control using experimental design strategies and a summarized electropolishing model. Electrochimica Acta. v. 53, p. 3356-3363, 2008.

LIU, Y.; CAO, X.; SHI, J.; SHEN, B.; HUANG, J.; HU, J.; CHEN, Z.; LAI, Y. A superhydrophobic TPU/CNTs@SiO_2 coating with excellent mechanical durability and chemical stability for sustainable anti-fouling and anti-corrosion. Chemical Engineering Journal. v. 434, 134605, 2022.

LIPPINCOTT, E. R.; VAN VALKENBURG, A.; WEIR, C.E.; BUNTING, E. N. Infrared Studies on Polymorphs of Silicon Dioxide and Germanium Oxide. Journal of Research of the National Bureau of Standards. v. 61, no. 1, p. 61-70, 1958.

MEDIAVILLA, M.; CASTRO, C.; CAPELLÁN, I.; MIGUEL, L.J.; ARTO, I.; FRECHOSO, F. The transition towards renewable energies: Physical limits and temporal conditions. Energy Policy. v. 52, p. 297-311, 2013.

OLIVEIRA, A. S. Avaliação da influência de tratamentos superficiais na absortância e morfologia de filmes absorvedores de Mo/SiO_2 obtidos via sputtering. Dissertation (Master in Renewable Energies) – Federal University of Paraíba, João Pessoa, 2021.

PALERMO, V.; MERINO, M. C. G.; VAZQUEZ, P.; ALONSO, J. A.; ROMANELLI, G.; RODRIGUEZ, M.; LASSA, S. Studies on structural, morphological, and optical properties of Cr_2O_3 nanoparticles synthesized via one step combustion process by different fuels. Matter. v. 24, no. 3, 2019.

QIAO, G.; WANG, S.; WANG, X.; CHEN, X.; WANG, X.; CUI, H. Preparation and corrosion protection performance of a pulse co-deposited Ni/Co/SiO_2 hydrophobic composite coating. ChemPhysMater. 2021.

RABAIA, M. K. H.; ABDELKAREEM, M. A.; SAYED, E. T.; ELSAID, K.; CHAE, K.-J.; WILBERFORCE, T.; OLABI, A. G. Environmental impacts of solar energy systems: A review. Science of The Total Environment. v. 754, 2021.

RANI, E.; INGALEA, A.; PHASEC, D.M.; CHATURVEDID, A.; MUKHERJEEB, C.; JOSHI, M.P.; KUKREJAB, L. M. Band gap tuning in Si-SiO_2 nanocomposite: Interplay of confinement effect and surface/interface bonding. Applied Surface Science. v. 425, p. 1089-1094, 2017.

RAUT, H.K.; GANESH, V.A.; NAIR, A.S.; RAMAKRISHNA, S. Anti-reflective coatings: A critical, in-depth review. Energy & Environmental Science. v. 4, p. 3779-3804, 2011.

SCHÄDLE, T.; PEJCIC, B.; MIZAIKOFF, B. Monitoring dissolved carbon dioxide and methane in brine environments at high pressure using IR-ATR spectroscopy. Analytical Methods. v. 8, no. 4, p. 756-762, 2016.

SILVA NETO, J. F. Development of Selective Surfaces for Solar Collectors with Multilayer Deposition of Cr and SiO_2. Thesis (Doctorate in Mechanical Engineering) – Federal University of Paraíba, João Pessoa, 2017.

ŠEST, E.; DRAŽIČ, G.; GENORIO, B.; JERMAN, I. Graphene nanoplatelets as an anticorrosion additive for solar absorber coatings. Solar Energy Materials and Solar Cells. v. 176, p. 19-29, 2018.

TABOR, H. Solar collectors, selective surfaces and heat engines. Proceedings of the National Academy of Sciences of the United States of America. v. 47, p. 1271-1278, 1961.

TSEGAY, M.G.; GEBRETINSAE, H.G.; NURU, Z. Y. Structural and optical properties of green synthesized Cr_2O_3 nanoparticles. Materials Today: Proceedings. v. 36, p. 587-590, 2021.

XU, K.; DU, M.; HAO, L.; MI, J.; YU, Q.; LI, S. A review of high-temperature selective absorbing coatings for solar thermal applications. Journal of Materiomics. v. 6(1), p. 167-182, 2020.

YU, H.; XU, X.; ZHANG, Y.; ZHANG, Q.; LI, G.; YAN, H. Preparation of high corrosion resistant solar absorbing coating on the surface of ferritic stainless steel by utilizing chemical coloring. Materials Letters. v. 270, 127628, 2020.

ZHANG, K.; HAO, L.; DU, M.; MI, J.; WANG, J.-N.; MENG, J.-P. A review on thermal stability and high temperature induced ageing mechanisms of solar absorber coatings. Renewable and Sustainable Energy Reviews. v. 67, p. 1282-1299, 2017.

7. RESPONSIBILITY NOTICE

The authors are the only responsible for the printed material included in this paper.